JOC*Article*

A Class II Aldolase Mimic

Jimmy Hedin-Dahlström, Jenny P. Rosengren-Holmberg, Sacha Legrand, Susanne Wikman, and Ian A. Nicholls*

Bioorganic and Biophysical Chemistry Laboratory, Department of Chemistry and Biomedical Sciences, University of Kalmar, SE-391 82 Kalmar, Sweden

ian.nicholls@hik.se

Received March 20, 2006

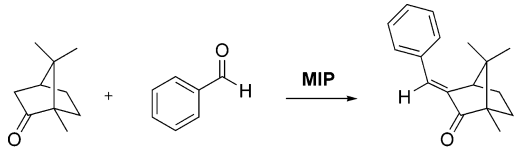

1a **2** **3a**

A class II aldolase-mimicking synthetic polymer was prepared by the molecular imprinting of a complex of cobalt (II) ion and either (1*S*,3*S*,4*S*)-3-benzoyl-1,7,7-trimethylbicyclo[2.2.1]heptan-2-one (**4a**) or (1*R*,3*R*,4*R*)-3-benzoyl-1,7,7-trimethylbicyclo[2.2.1]heptan-2-one (**4b**) in a 4-vinylpyridine−styrene−divinylbenzene copolymer. Evidence for the formation of interactions between the functional monomer and the template was obtained from NMR and VIS titration studies. The polymers imprinted with the template demonstrated enantioselective recognition of the corresponding template structure, and induced a 55-fold enhancement of the rate of reaction of camphor (**1**) with benzaldehyde (**2**), relative to the solution reactions, and were also compared to reactions with a series of reference polymers. Substrate chirality was observed to influence reaction rate, and the reaction could be competitively inhibited by dibenzoylmethane (**6**). Collectively, the results presented provide the first example of the use of enantioselective molecularly imprinted polymers for the catalysis of carbon−carbon bond formation.

Introduction

The development of new methodologies for the catalysis of carbon−carbon bond formation remains one of the greatest challenges for organic chemistry.[1] The desire to produce systems mimicking those demonstrated by biological macromolecular catalysts, i.e., enzymes[2] and ribozymes,[3] requires not just a capacity to enhance the rate of a given reaction, but also that the system can provide some control over substrate selectivities and display turnover. These additional goals exacerbate the complexity of the task. Nonetheless, a number of quite diverse strategies have been utilized in order to produce biomimetic systems capable of catalyzing C−C bond formation,[4] including the use of chiral Lewis acids,[5] catalytic antibody technology,[6] and molecular imprinting.[7]

The molecular imprinting technique[8] provides a means for the synthesis of functionally and stereochemically defined environments in which to perform selective reactions.[7,9] The inherent stability of these highly cross-linked polymers makes them of particular interest for applications where extremes of

* Address correspondence to this author. Phone: +46-480 446258. Fax: +46-480 446244.

(1) (a) Danishefsky, S. *Science* **1993**, *259*, 469−470. (b) Sukumaran, J.; Hanefeld, U. *Chem. Soc. Rev.* **2005**, *34*, 530−42.

(2) (a) Bornscheuer, U. T.; Kazlauskas, R. J. *Angew. Chem., Int. Ed.* **2004**, *43*, 6032−6040. (b) Jaeger, K.-E.; Eggert, T. *Curr. Opin. Biotechnol.* **2004**, *15*, 305−313.

(3) (a) Lilley, D. M. J. *Curr. Opin. Struct. Biol.* **2005**, *15*, 313−323. (b) Sigel, R. K. O. *Eur. J. Inorg. Chem.* **2005**, *12*, 2281−2292.

(4) Severin, K. *Curr. Opin. Chem. Biol.* **2000**, *4*, 710−714.

(5) Mastrorilli, P.; Nobile, C. F. *Coord. Chem. Rev.* **2004**, *248*, 377−395.

(6) Schultz, P. G.; Yin, J.; Lerner, R. A. *Angew. Chem., Int. Ed.* **2002**, *41*, 4427−4437.

(7) Alexander, C.; Davidson, L.; Hayes, W. *Tetrahedron* **2003**, *59*, 2025−2057.

(8) (a) Sellergren, B., Ed. *Molecularly Imprinted Polymers. Man-made Mimics of Antibodies and Their Applications in Analytical Chemistry*; Elsevier: Amsterdam, The Netherlands, 2001. (b) Yan, M.; Ramström, O., Eds. *Molecularly Imprinted Materials. Science and Technology*; Marcel Dekker: New York, 2005. (c) Alexander, C.; Andersson, H. S.; Andersson, L. I.; Ansell, R. J.; Kirsch, N.; Nicholls, I. A.; O'Mahony, J.; Whitcombe, M. J. *J. Mol. Recognit.* **2006**, *19*, 106−180.

(9) (a) Whitcombe, M. J.; Alexander, C.; Vulfson, E. N. *Synlett* **2000**, *6*, 911−923. (b) Motherwell, W. B.; Bingham, M. J.; Six, Y. *Tetrahedron* **2001**, *57*, 4663−4686. (c) Bruggemann, O. *Anal. Chim. Acta* **2001**, *435*, 197−207. (d) Tada, M.; Iwasawa, Y. *J. Mol. Catal. A* **2003**, *199*, 115−137. (e) Toorisaka, E.; Uezu, K.; Goto, M.; Furusaki, S. *Biochem., Eng. J.* **2003**, *14*, 85−91. (f) Striegler, S. *J. Chromatogr. B* **2004**, *804*, 183−195. (g) Cheng, Z. Y.; Zhang, L. W.; Li, Y. Z. *Chem. Eur. J.* **2004**, *10*, 3555−3561.

10.1021/jo060608b CCC: $33.50
Published on Web 06/02/2006

SCHEME 1. Aldol Condensation between (*S*)-Camphor (1a) and Benzaldehyde (2) Results in Formation of (*S*)-3-Benzylidenecamphor (3a) and the Same Reaction with (*R*)-Camphor (1b) Results in Formation of (*R*)-3-Benzylidenecamphor (3b)

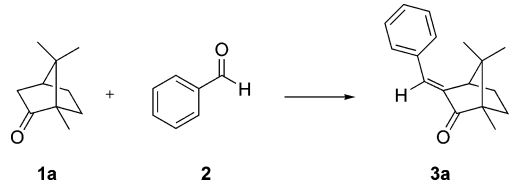

temperature, solvent regime, or pH prohibit the use of catalysts of biological origin.[10] The technique has been used with success for preparing polymers capable of enhancing the reaction rate of a number of types of reactions including various hydrolytic reactions,[11] transamination,[12] and β-elimination.[13] Previous efforts to develop systems for the catalysis of C−C bond forming reactions have been reported by us, aldol condensation,[14] and others, Diels−Alder cyclization[15] and the Suzuki reaction.[16]

The aldol condensation is a reaction of central importance to both biology[17,18] and synthetic organic chemistry.[19,20] Accordingly, significant effort has been directed to the development of catalysts for this class of reaction, and to the establishment of means for controlling the stereochemistry of the reaction outcome, e.g., Evans' oxazolidinones,[21] catalytic antibodies,[22] chiral Lewis acids,[23] and molecular imprinting.[14]

In the present study we report the design, synthesis, and evaluation of enantioselective molecularly imprinted polymers with activity mimicking that of a class II aldolase, a metalloenzyme found in lower organisms such as bacteria and yeast.[24] The reaction of (*S*)- or (*R*)-camphor (**1**) and benzaldehyde (**2**) to yield the corresponding (*E*)-3-benzylidene-1,7,7-trimethylbicyclo[2.2.1]heptan-2-one (**3**) was chosen for use in this study (Scheme 1). The diketones **4** and **5** (Figure 1) were envisaged as putative analogues for the transition state for the first step of this Co^{2+} catalyzed aldol condensation reaction. Furthermore, the diketone functionalities, or keto−enol tautomers thereof,

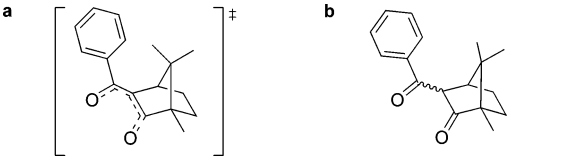

FIGURE 1. (a) Proposed transition state (TS) for the first step of the aldol condensation reaction. (b) General structure of the putative (*S*)-TSAs: *exo* (**4a**) and *endo* (**5a**). The corresponding (*R*)-TSAs are defined as **4b** (*exo*) and **5b** (*endo*).

should also serve as suitable ligands for coordination to the metal ion. Molecularly imprinted polymers synthesized by using complexes of **4** with Co^{2+} in a 4-vinylpyridine (4-VP)−styrene−divinylbenzene (DVB) copolymer demonstrated significant enhancement of the rate of reaction relative to reference polymers and the solution reaction. Moreover, polymers synthesized with either enantiomer of **4** displayed selectivity for substrate structures of the corresponding optical antipode.

Results and Discussion

The enantioselective synthetic aldolase-mimicking polymers presented in this study were designed and synthesized by using a metal ion mediated molecular imprinting strategy. The reaction chosen for investigation involves the condensation of camphor (**1**) and benzaldehyde (**2**) in the presence of a mild base, pyridine, to yield 3-benzylidenecamphor (**3**) (Scheme 1). The choice was in part due to the inherent chirality present in camphor, and in part due to the presence of a single hydrogen-bearing α-carbon, which provides a natural limit to the number of possible reaction products. Camphor's chirality has previously been utilized for steering the stereochemical outcome of aldol reactions employing titanium enolates of camphorselenoacetone and methyl camphorselenoacetate,[25] and for a range of other asymmetric syntheses[26] involving diols and aminodiols[27] and lithium enolates of α-hydroxy ketones.[28]

Design and Synthesis of Transition State Analogues. The choice of the putative TSAs (**4** and **5**) proposed for use in this study was based upon our previous experience with a related aldolase mimicking polymer selective for the production of chalcone (**8**),[14] whereby complexes of the TSA with Co^{2+} would provide a mimic for the transition state of the aldol reaction (Scheme 1, Figure 1). This bidentate ligand was expected to

(10) Svenson, J.; Nicholls, I. A. *Anal. Chim. Acta* **2001**, *435*, 19−24.
(11) (a) Strikovsky, A. G.; Kasper, D.; Grün, M.; Green, B. S.; Hradil, J.; Wulff, G. *J. Am. Chem. Soc.* **2000**, *122*, 6295−6296. (b) Wulff, G.; Gross, T.; Schönfeld, R. *Angew. Chem., Int. Ed. Engl.* **1997**, *36*, 1961−1964. (c) Sellergren, B.; Shea, K. J. *Tetrahedron*: *Asymmetry* **1994**, *5*, 1403−1406. (d) Sellergren, B.; Karmalkar, R. N.; Shea, K. J. *J. Org. Chem.* **2000**, *65*, 4009−4027.
(12) Svenson, J.; Zheng, N.; Nicholls, I. A. *J. Am. Chem. Soc.* **2004**, *126*, 8554−8560.
(13) (a) Müller, R.; Andersson, L. I.; Mosbach, K. *Makromol. Chem.-Rapid Commun.* **1993**, *14*, 637−641. (b) Beach, J. V.; Shea, K. J. *J. Am. Chem. Soc.* **1994**, *116*, 379−380.
(14) Matsui, J.; Nicholls, I. A.; Karube, I.; Mosbach, K. *J. Org. Chem.* **1996**, *61*, 5414−5417.
(15) (a) Liu, X.-C.; Mosbach, K. *Macromol. Rapid Commun.* **1997**, *18*, 609−615. (b) Visnjevski, A.; Schomäcker, R.; Yilmaz, E.; Brüggemann, O. *Catal. Commun.* **2005**, *6*, 601−606. (c) Busi, E.; Basosi, R.; Ponticelli, F.; Olivucci, M. *J. Mol. Catal. A*: *Chem.* **2004**, *217*, 31−36.
(16) Cammidge, A. N.; Baines, N. J.; Bellingham, R. K. *Chem. Commun.* **2001**, 2588−2589.
(17) Mikami, K.; Yajima, T.; Takasaki, T.; Matsukawa, S.; Terada, M.; Uchimaru, T.; Maruta, M. *Tetrahedron* **1996**, *52*, 85−98.
(18) Mahrwald, R., Ed. *Modern Aldol Reactions*, *Vol. 1*: *Enolates, Organocatalysis, Biocatalysis and Natural Product Synthesis*; Wiley-VCH Verlag GmbH & Co., KGaA: Weinheim, Germany, 2004.
(19) Machajewski, T. D.; Wong, C.-H. *Angew. Chem., Int. Ed.* **2000**, *39*, 1352−1374.
(20) Mahrwald, R., Ed. *Modern Aldol Reactions*, *Vol. 2*: *Metal Catalysis;* Wiley-VCH Verlag GmbH & Co., KGaA: Weinheim, Germany, 2004.
(21) (a) Evans, D. A.; Kim, A. S. In *Handbook of Reagents for Organic Synthesis*: *Reagents, Auxiliaries and Catalysts for C−C Bonds*; Coates, R. M., Denmark, S. E., Eds.; John Wiley & Sons: New York, 1999; pp 91−101. (b) Evans, D. A.; Bartroli, J.; Shih, T. L. *J. Am. Chem. Soc.* **1981**, *103*, 2127−2129. (c) Evans, D. A.; Nelson, J. V.; Taber, T. R. *Top. Stereochem.* **1982**, *13*, 1−115.
(22) (a) Hoffmann, T.; Zhong, G.; List, B.; Shabat, D.; Anderson, J.; Gramatikova, S.; Lerner, R. A.; Barbas, C. F., III *J. Am. Chem. Soc.* **1998**, *120*, 2768−2779. (b) Zhong, G.; Lerner, R. A.; Barbas, C. F., III *Angew. Chem., Int. Ed.* **1999**, *38*, 3738−3741.
(23) (a) Calter, M. A.; Song, W.; Zhou, J. G. *J. Org. Chem.* **2004**, *69*, 1270−1275. (b) Saito, S.; Yamamoto, H. *Acc. Chem. Res.* **2004**, *37*, 570−579.
(24) Heron, E. J.; Caprioli, R. M. *Biochim. Biophys. Acta* **1975**, *403*, 563−572.
(25) Tiecco, M.; Testaferri, L.; Marini, F.; Sternativo, S.; Santi. C.; Bagnoli, L.; Temperini, A. *Tetrahedron*: *Asymmetry* **2004**, *15*, 783−791.
(26) Knollmuller, M.; Ferencic, M.; Gärtner, P.; Mereiter, K.; Noe, C. R. *Tetrahedron*: *Asymmetry* **1998**, *9*, 4009−4020.
(27) Palomo, C.; Oiarbide, M.; Aizpurua, J. M.; González, A.; García, J. M.; Landa, C.; Odriozola, I.; Linden, A. *J. Org. Chem.* **1999**, *64*, 8193−8200.
(28) Palomo, C.; Oiarbide, M.; Mielgo, A.; González, A.; García, J. M.; Landa, C.; Lecumberri, A.; Linden, A. *Org. Lett.* **2001**, *3*, 3249−3252.

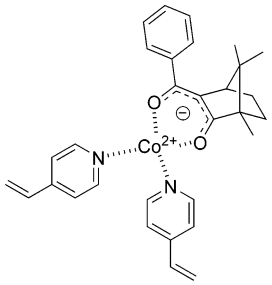

FIGURE 2. Proposed metal (Co^{2+}) ion coordinated complex formation between the enolate of the TSA (**4** or **5**), Co^{2+}, and 4-vinylpyridine, showing four of six possible coordinating functionalities.

fill two of the coordination sites of the Co^{2+} using its two oxygens, while 4-vinylpyridine (and/or solvent) should fill the remaining sites of the Co^{2+} complex (Figure 2). It was envisaged that the keto−enol tautomerism available to the β-diketones would allow for a planar geometry between the two oxygens, as would also be the case in the corresponding enolate and its various tautomers (see the Supporting Information).

The use of metal ions in molecular imprinting protocols can provide a number of advantages in the preparation of synthetic receptors[29] and enzyme mimics.[14,30] The general strengths of transition metal ion−ligand coordination interactions can permit complex formation in polar solvents not normally conducive for use in noncovalent molecular imprinting strategies. Furthermore, the possibility for forming multiple interactions to a single ion allows for the simultaneous coordination of multiple ligands, e.g., reaction substrates.

The synthesis of each of the enantiomers of the diketones **4** and **5** was undertaken in order to obtain material for use in the polymer syntheses and for polymer−ligand recognition studies. The *exo*-products, **4a** and **4b**, were obtained in moderate yield, as the exclusive products from the treatment of the corresponding enantiomer of camphor (**1a** or **1b**) with NaH and ethyl benzoate (Scheme 2), using an adaption of a procedure previously described by Togni.[31]

The benzoyl substituent of **4a** was found to be in the *exo*-configuration on the basis of the observed NOESY correlations arising from the H^{α} positioned between the two carbonyls and the two CH_{endo} protons (Figure 3). The ^1H NMR spectra of **4a** (or **4b**) revealed an equilibrium between the diketo form and the two keto−enol forms, with a ratio of 3 to 7 in favor of the diketone. Partial assignment of the ^1H and ^{13}C NMR spectra was accomplished by the application of a combination of conventional 1D and 2D NMR experiments.

SCHEME 2. Synthesis of Diketone 4a from (*S*)-Camphor (1a)[a]

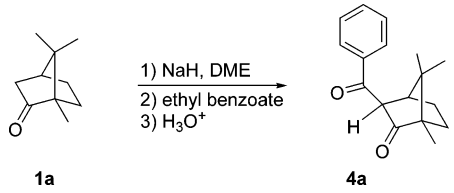

[a] Diketone **4b** was obtained from (*R*)-camphor (**1b**), using the same reaction conditions.

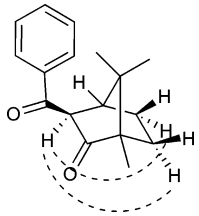

FIGURE 3. The dashed lines represent selected observed NOESY correlations of **4a**. The same correlations were observed for **4b**.

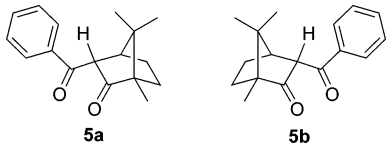

FIGURE 4. Structure of the endo diketones **5a** and **5b**.

SCHEME 3. Synthesis of the Diketones 5a and 4a from 7a

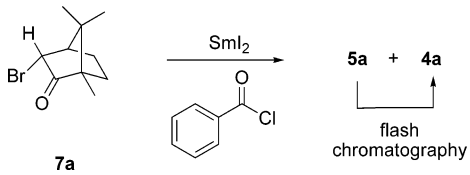

Attempts were made to obtain the corresponding *endo*-isomers, the diketones **5a** and **5b** (Figure 4), using a procedure described by Wei et al.[32] in order to provide alternative analytes for use in polymer−ligand recognition studies. The ^1H NMR spectra of the crude products arising from the treatment of bromocamphor, **7a**, with SmI_2 in the presence of benzoyl chloride under samarium-Barbier conditions[33] demonstrated a peak characteristic of the *endo* H^{α} (doublet at 2.85−2.83 ppm) of **4a**. Furthermore, a doublet of doublets was observed at 4.25 ppm corresponding to the signal of the *exo* H^{α} to the carbonyl moieties present in **5a**. This was interpreted as being indicative of the presence of a mixture of the *exo*-diketone **4a** and the *endo*-diketone **5a** (Scheme 3), in a 2:1 ratio in favor of **4a**. Attempts to separate **5a** from **4a** by flash chromatography on silica failed to achieve separation, irrespective of matrix (neutral, acidic, or basic), as shown by the disappearance of the doublet of doublets at 4.25 ppm in the ^1H NMR spectrum. This implied that the *exo*-product is the thermodynamically more stable of the two, and that the initial mixture reflects the presence of both kinetic (*endo*) and thermodynamic (*exo*) products, for which keto−enol tautomerism provides a mechanism for interchange between the two (Figure 5, see also the Supporting Information

(29) (a) Gupta, S. N.; Neckers, D. C. *J. Polym. Sci., Polym. Chem. Ed.* **1982**, *20*, 1609−1622. (b) Vidyasankar, S.; Ru, M.; Arnold, F. H. *J. Chromatogr. A* **1997**, *775*, 51−63. (c) Hart, B. R.; Shea, K. J. *J. Am. Chem. Soc.* **2001**, *123*, 2072−2073. (d) Takeuchi, T.; Mukawa, T.; Matsui, J.; Higashi, M.; Shimizu, K. D. *Anal. Chem.* **2001**, *73*, 3869−3874. (e) Efendiev, A. A. *Macromol. Symp.* **1994**, *80*, 289−313. (f) Matsui, J.; Nicholls, I. A.; Takeuchi, T.; Mosbach, K.; Karube, I. *Anal. Chim. Acta* **1996**, *335*, 71−77. (g) Fujii, Y.; Matsutani, K.; Kikuchi, K. *J. Chem. Soc., Chem. Commun.* **1985**, 415−417. (h) Dhal, P. K.; Arnold, F. H. *J. Am. Chem. Soc.* **1991**, *113*, 7417−7418. (i) Striegler, S.; Tewes, E. *Eur. J. Inorg. Chem.* **2002**, 487−495. (j) Striegler, S. *Anal. Chim. Acta* **2005**, *539*, 91−95. (k) Striegler, S.; Dittel M. *Anal. Chim. Acta* **2003**, *484*, 53−62.

(30) (a) Brunkan, N. M.; Gagné, M. R. *J. Am. Chem. Soc.* **2000**, *122*, 6217−6225. (b) Santora, B. P.; Larsen, A. O.; Gagné, M. R. *Organometallics* **1998**, *17*, 3138−3140. (c) Koh, J. H.; Larsen, A. O.; White, P. S.; Gagné, M. R. *Organometallics* **2002**, *21*, 7−9. (d) Wulff, G.; Vietmeier, J. *Makromol. Chem. − Macromol. Chem. Phys.* **1989**, *190*, 1727−1735. (e) Leonhardt, A.; Mosbach, K. *React. Polym.* **1987**, *6*, 285−290.

(31) Togni, A. *Organometallics* **1990**, *9*, 3106−3113.

(32) Wei, H.-X.; Wang, Z.-M.; Shi, M. *Chem. Pharm. Bull.* **1999**, *47*, 909−910.

(33) Namy, J. L.; Girard, P.; Kagan, H. B. *Nouv. J. Chim.* **1977**, *1*, 5−7.

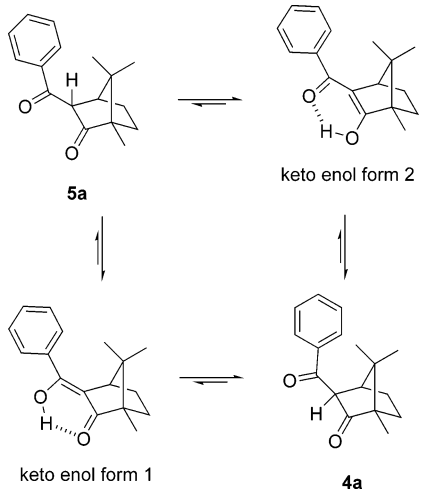

FIGURE 5. Isomerization of **5a** to **4a**.

SCHEME 4. Synthesis of Ketone 3a from (*S*)-Camphor (1a)[a]

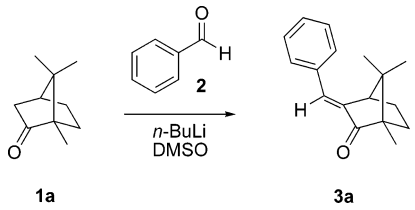

[a] Ketone **3b** was synthesized from **1b** in the same manner.

for a proposed mechanism). Identical behavior was observed in the synthesis of **5b** from **7b**, which resulted in isomerization to the more favored **4b**. Collectively, the results provide an important insight into the behavior of the diketones, namely that the keto−enol tautomerism demonstrated by the diketones provides evidence that the TSAs can adopt a planar geometry, as proposed for a suitable TSA.

Synthesis of Aldol Condensation Products. The products from the aldol condensation, the α,β-unsaturated ketones **3a** and **3b**, were synthesized for use in the establishment of assays and as standards for polymer−ligand recognition studies, using an adaption of the procedure described by Chuiko et al.[34] Enantiomerically pure camphor, **1a** or **1b**, was reacted with benzaldehyde (**2**) in the presence of *n*-BuLi in DMSO to furnish the corresponding ketone, **3a** or **3b**, though in low yield (Scheme 4).

NOESY experiments with **3a** (or **3b**) showed a strong correlation between the H^4 methine and the H^{3d} aromatic protons (Figure 6), suggesting an (*E*)-configuration. The lack of any observed correlation between H^4 and H^{3b} supported this conclusion.

Template−Monomer Complexation Studies. Initial studies on the solubility of $Co(OAc)_2$ suggested the use of methanol as a suitable solvent for the polymerization reactions. This protic solvent is not normally suitable for use in noncovalent molecular imprinting protocols; however, in this case the significant strength of metal ion coordination surmounts the competition from bulk solvent. A series of VIS and NMR titration studies (see the Supporting Information) were performed to establish

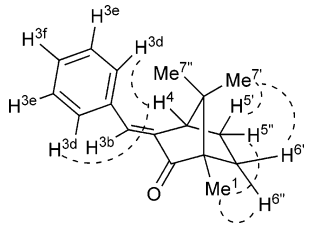

FIGURE 6. The dashed lines represent selected NOESY correlations of the unsaturated ketone **3a**.

the presence and strength of complexes between Co^{2+}, TSA (**4a** or **4b**), and pyridine (here used as an analogue for 4-VP). The monitoring of titrations of Co^{2+} with pyridine or TSA at 520 nm (294 ± 1 K) revealed complexes with apparent dissociation constants (app K_{diss}) of 228.9 ± 18.3 and 4.0 ± 1.6 mM, respectively. By using conditions and concentrations comparable to those used (see later) in the polymerization reaction, namely using 2 equiv of pyridine per Co^{2+}, an app K_{diss} of 25.6 ± 3.8 mM was determined, indicating that the TSA can compete for coordination of the metal ion. These data were supported by ^1H NMR studies, from which an app K_{diss} of 2.50 ± 0.39 mM was determined by following the downfield shift of the H^{α}. Complementary VIS studies with Job's method of continuous variation[35,36] demonstrated a 1:1 stoichiometry for the solution complexes of Co^{2+} and **4**. On the basis of molecular model studies, we propose that the steric bulk of **4** excludes the formation of complexes of greater than 1:1 complex stoichiometry under the conditions studied. On account of the complex stabilities described above, we interpret the favorable formation of 1:1:2 complexes of Co^{2+}/TSA/pyridine, relative to 1:2 complexes of Co^{2+}/TSA on account of the relative bulk of the TSA. Importantly, these results collectively demonstrate that complexes of Co^{2+} by pyridine and TSA are formed at the concentrations utilized in subsequent polymerization reactions. The role of Co^{2+} in the complex is 2-fold, in the first instance to provide coordination of the template during the molecular imprinting process, and second to facilitate binding of reaction substrates in the subsequent polymer.

Polymer Synthesis and Characterization. A series of 4-vinylpyridine−styrene−divinylbenzene copolymers were synthesized by thermally induced radical polymerization with use of azobis(cyclohexanecarbonitrile) (ABCC) as initiator (Table 1). Two polymers, one prepared in the absence of both template (TSA) and Co^{2+} (**P0**) and another prepared in the presence of Co^{2+} but without TSA (**P1**), were synthesized to act as references for polymers prepared by using complexes of the (*S*)- and (*R*)-TSA with Co^{2+}, (**P2**) and (**P3**), respectively. The two reference polymers were anticipated to provide insight regarding the influence of the polymer material itself on ligand recognition (**P0**) and the role of sites selective for cobalt ions (**P1**). In the case of **P3**, its physical and chemical characteristics were effectively identically with those of **P2**, though with selectivity for the (*R*)-TSA (**4b**) and (*R*)-product (**3b**). Moreover, no evidence of residual template was evident based upon examination of the carbonyl region of FT-IR spectra.

(34) Chuiko, V. A.; Vinarskaya, Z. V.; Izotova, L. V.; Tychinskaya, L. Y. *Russ. J. Org. Chem.* **2002**, *38*, 196−199.

(35) (a) Kim, H.; Spivak, D. A. *J. Am. Chem. Soc.* **2003**, *125*, 11269−11275. (b) Takeuchi, T.; Dobashi, A.; Kimura, K. *Anal. Chem.* **2000**, *72*, 2418−2422. (c) Striegler, S. *Bioseparation* **2001**, *10*, 307−314. (d) Wulff, G.; Knorr, K. *Bioseparation* **2001**, 10, 257−276.

(36) Karlsson, J. G.; Andersson, L. I.; Nicholls, I. A. *Anal. Chim. Acta* **2001**, *435*, 57−64.

TABLE 1. Polymerization Reaction Mixture Compositions and Polymer Physical Characterization

	P0[a]	P1[b]	P2[c]	P3[d]
(*S*)-TSA **4a** (mmol)			2.0	
(*R*)-TSA **4b** (mmol)				2.0
$Co(OAc)_2$ (mmol)		2.0	2.0	2.0
4-VP (mmol)	4.0	4.0	4.0	4.0
styrene (mmol)	40.0	40.0	40.0	40.0
DVB (mmol)	40.0	40.0	40.0	40.0
ABCC (mmol)	1.2	1.2	1.2	1.2
MeOH (ml)	14.98	14.98	14.98	14.98
% C found (theoretical: 91.5)	91.8	90.0	89.5	89.8
% H found (theoretical: 7.7)	8.1	7.9	7.7	7.7
% N Found (theoretical: 0.7)	0.8	0.8	0.8	0.8
BET surface area ($m^2\ g^{-1}$)	1.9	3.4	3.5	3.9
micropore volume ($cm^3\ g^{-1}$)	0.005	0.009	0.009	0.010
average pore diameter (Å)	111.0	104.6	104.4	103.4

[a] Reference polymer. [b] Co^{2+} reference polymer. [c] (*S*)-TSA imprinted polymer. [d] (*R*)-TSA imprinted polymer.

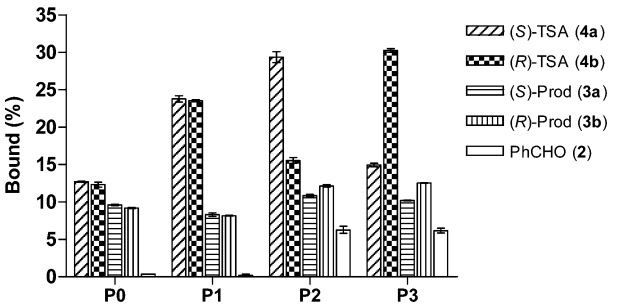

FIGURE 7. Binding of the 0.015 mM ligand:cobalt complex (1:1) in MeOH. Each experiment was performed in duplicate with duplicate HPLC analyses of each sample. Error bars reflect the SD. (Figures and uncertainties underlying the data presented in this graph are presented in the Supporting Information, along with results of binding in DMF.)

Evaluation of Polymer−Ligand Recognition. An assay for TSA binding to the polymers was developed based upon a series of polymer titration studies performed with established procedures (data not shown).[36] A polymer concentration of 20 mg mL^{-1} was chosen for use in the investigation of polymer−template rebinding in batch binding experiments performed in MeOH (Figure 7).

In the case studies performed in MeOH, using **P0**, a polymer devoid of the influence of both TSA and Co^{2+} on the polymer's recognition characteristics, some preference for binding of the TSAs was observed relative to the single carbonyl containing products (**3a** and **3b**), though not surprisingly without any enantioselectivity. The structurally smaller substrate, benzaldehyde (**2**), demonstrated effectively no recognition of the polymer. In the case of the polymer synthesized in the presence of Co^{2+}, **P1**, the presence of sites selective for the cation significantly enhanced recognition of the TSA relative to that observed in **P0**, though no significant effect was seen on the binding of **2** or **3** (**a** or **b**). This is interpreted as resulting from the presence of sites selective for Co^{2+}, in which the bound ions in turn facilitate coordination of the diketone **4**.

The (*S*)-TSA imprinted polymer **P2** showed similar affinities to **3** (**a** or **b**) as seen in the case of **P1**, though a substantial increase in affinity for benzaldehyde (**2**). Importantly, an increased preference for the (*S*)-TSA **4a**, relative to **4b**, was observed, which provides strong evidence for the presence of sites with selectivity for the (*S*)-enantiomer of the TSA (**4a**).

TABLE 2. Binding of Co^{2+} to Polymers after Incubation in MeOH

polymer	bound[a] (mM)	*n* (μmol/g polymer)
P0	0.155 ± 0.149	0.776 ± 0.747
P1	1.352 ± 0.150	6.762 ± 0.747
P2	0.542 ± 0.001	2.710 ± 0.004
P3	0.543 ± 0.100	2.713 ± 0.498

[a] Incubation with Co^{2+} solution (8 mM) in MeOH (293 K), experiments performed in duplicate with duplicate analyses.

Polymer **P3**, prepared with (*R*)-TSA (**4b**), behaved similarly, though as expected with a reversal in enantioselectivity. Under the conditions studied, the enantioselective binding correlates to 0.11 μmol enantioselective sites per gram of polymer, i.e., the difference between the binding of **4a** and **4b** to **P2**, or **P3**. The ratio of enantiomer binding correlates to a difference in free energy of binding between the two enantiomers ($\Delta\Delta G$) of 1.6 kJ mol^{-1}.[12,37] Although a significant difference, the results illustrate the site heterogeneity present inherent to **P2** and **P3**. Binding studies were also performed in DMF at 293 ± 2 K (see the Supporting Information), which was the solvent of choice for use in studies on the influence of the polymers on reaction kinetics. In DMF the polymers demonstrated greater affinities for the template structure, in particular **P0**, though with no enantioselectivity. Interestingly, and in contrast to the results obtained in MeOH, no significant product binding was observed, though benzaldehyde (**2**) displayed a markedly greater affinity for the polymers, especially in the case of **P1**.

As the metal ion plays a fundamental role in the catalysis of the aldol reaction used in this study,[14,38] it was crucial to determine the quantity of Co^{2+} that bound to the polymers. Batch binding studies (Table 2) showed that the polymer synthesized with Co^{2+} as template, **P1**, had a significantly greater capacity for rebinding the divalent cation than that with **P2**, or **P3**. This was interpreted as reflecting the presence of sites selective for Co^{2+} rather than for Co^{2+}−TSA complexes where in principle coordinating moieties, the two ketones, are lacking in the resultant polymer. Interestingly, **P0** showed an even lower capacity than the other polymers. This is attributed to the lack of a template, which renders the polymer without ensembles of pyridinyl functionalities in suitable spatial arrangements for simultaneous interaction with the metal ion.

Reaction Kinetics Studies. The influence of the various polymers on the rate of condensation of benzaldehyde (**2**) and (*S*)- or (*R*)-camphor (**1a**, **1b**) was studied by using reactions performed in sealed tubes with DMF as solvent and elevated temperature (100 °C). Polymers were charged with methanolic Co^{2+} solutions prior to use (Table 2). A solvent reaction containing pyridine and $Co(OAc)_2$ was employed to allow assessments of the influence of the polymers themselves. Since the binding of cobalt to **P0** was quite low, studies with this polymer employed Co^{2+} concentrations identical with those of the solvent reaction. An HPLC-based assay was used to monitor the formation of reaction products **3a** or **3b** (Figure 8). To provide a clear picture of the role of the polymer on the reaction studied, product yields are presented as yield per mole sites, where the number of sites was determined by the Co^{2+} concentration in the bound polymer. As stated earlier, the presence of the metal ion is essential for the reaction to proceed within the time frames studied.

(37) Adbo, K.; Nicholls, I. A. *Anal. Chim. Acta* **2001**, *435*, 115−120.
(38) Watanabe, K.; Imazawa, A. *Bull. Chem. Soc. Jpn.* **1982**, *55*, 3208−3211.

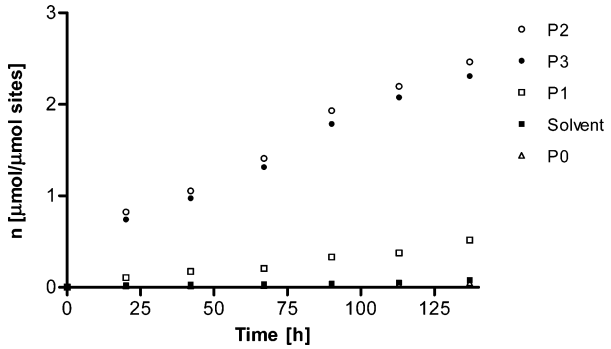

FIGURE 8. Formation of (*S*)-product (**3a**) per mol site (Co^{2+}), using (*S*)- (**P2**) and (*R*)-MIPs (**P3**), Co^{2+} (**P1**), and nonimprinted (**P0**) polymers, and solvent reaction (comparable to **P0**) and the corresponding solvent reaction. Data were obtained from duplicate experiments with each analysis performed in duplicate. Error bars (not discernible) reflect SEM < 0.01 μmol/μmol sites.

TABLE 3. Turnover per Co^{2+} for Production of 3a[a]

polymer	turnover (h^{-1})
P0	0.38×10^{-3}
P1	4.63×10^{-3}
P2	21.04×10^{-3}
P3	20.30×10^{-3}

[a] (*S*)-Product (**3a**) formation based on time course experiments of 160 h.

The time course studies show that the presence of **P0** has effectively no influence on the rate of reaction, as compared to the solution reaction performed with the same amount of Co^{2+} present (Figure 8 and Table 3). This implies that the polymer matrix itself does not induce rate enhancement. However, in the case of **P1**, which possesses sites selective for Co^{2+}, a 12-fold increase in reaction rate was obtained. This is attributed to the presence of sites capable of binding complexes of $Co^{2+}$and substrate, i.e., sites with incomplete coordination of the metal ion by the pyridinyl residues of the polymer allowing for access by the substrates. This line of reasoning is supported by the results obtained with **P2**, which increases reaction rate by a factor of 55 relative to the solution and **P0** reactions. Assays run with **P3**, with sites selective for the (*R*)-enantiomer of camphor (**1b**), were slightly slower suggesting either that the sites were not as well suited for accommodating the (*S*)-substrate, or that a small population of the sites are inaccessible to **1b** because of their high fidelity recognition of the (*S*)-configuration of the template. Importantly, reactions performed with **P3** and **1b** as substrate demonstrated the same reaction rate enhancements as observed for reactions with **P2** and **1a**. The poor stereochemical control of this reaction reflects the outcomes of studies by Gagné[30a−c] and Severin,[4] where lack of significant steric control around the reaction center may underlie the stereochemical outcome of the reactions studied. On account of the enantioselectivities observed in the binding studies, experiments were also performed (at reflux and room temperature) in MeOH, though no product was observed, most likely due to competition for sites at the metal ion, and/or quenching of any carbanion formed. Furthermore, differences between the gas accessible surface areas of these polymers are minimal, which allows us to exclude nonspecific surface effects as a basis for the observed rate enhancements. This is further supported by swelling studies performed in DMF (see the Supporting Information) which demonstrated no significant difference in the swelling characteristics of the polymers used in this study.

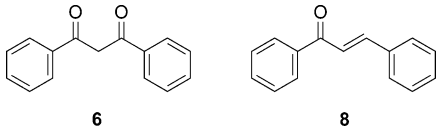

FIGURE 9. Structure of the inhibitor dibenzoylmethane (DBM) (**6**) and chalcone (**8**).

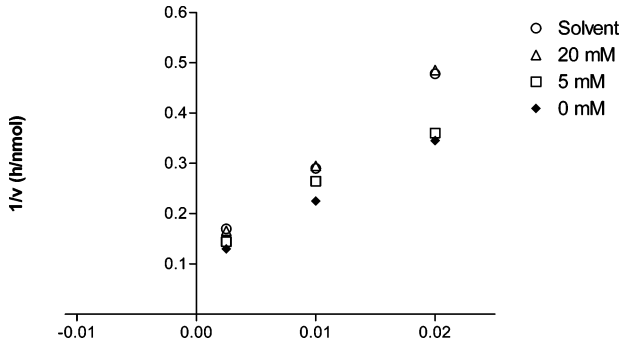

FIGURE 10. Lineweaver−Burk plot of the formation of (*S*)-product (**3a**) with and without the presence of an inhibitor (**6**), and the reaction in solvent.

Interestingly, the enantioselectivities observed in the binding studies were not apparent in the studies on the influence of the polymers on the outcome of the reaction of **1** and **2**. While the binding studies are performed under equilibrium conditions, i.e., thermodynamic control, the studies of the kinetics of the reaction are never under true equilibrium conditions as the number and type of potential ligands vying for the sites varies over time. The results from the kinetics studies indicate that the sites influencing enantioselectivity, perhaps those of highest affinity, are not as effectively utilized during the reaction as in binding studies. Comparable results have been obtained from other systems,[4,30c] which may reflect either higher levels of inhibition of these sites or that the higher affinity sites are less accessible and that mass transfer becomes a limiting factor. It is arguable that both factors could contribute to the observed results. Moreover, and specifically in terms of stereochemical control, the results may also reflect a lack of steric definition in the vicinity of the reaction center.

Studies on the influence of the enantiomers of the TSA itself (**4a** and **4b**) on the reaction were performed to examine the role of the imprinting sites on the reaction kinetics. However, the TSA was found to rapidly degrade under the conditions employed in the reaction assay. It is noteworthy that studies of TSA under polymerization conditions demonstrated it to be stable. Furthermore, the presence of the reaction products (**3a** or **3b**) demonstrated no significant influence on reaction rate. An alternative strategy was to use dibenzoylmethane (**6**, DBM) (Figure 9), which we have previously used as a TSA in related studies for catalyzing production of chalcone (**8**).[14] Reactions performed with methanol as solvent yield no product under the conditions employed; other solvent configurations shall be utilized in future studies. Although **6** has a benzyl group instead of the chiral camphor moiety, simple molecular model studies suggested that it could fit to the volume of **4a** and **4b**, and therefore should be able to access sites selective for the original TSAs. A concentration-dependent competitive inhibition of the reaction (V_{max}= 10.11 ± 0.03 nmol/h; K_m = 126.26 ± 0.96

mM; $K_i = 30.4 \pm 0.35$ mM) by DBM (**6**) was demonstrated (Figure 10). In the presence of 20 mM of **6**, the reaction rate is reduced to that of the solution reaction. The inhibition is indicative of the presence of sites selective for DBM which are necessary for the catalysis of the reaction.

Collectively, the rate enhancing influence of the TSA imprinted polymers, together with the concentration inhibitory effect of **6**, demonstrates that sites selective for the transition state analogue are responsible for the catalysis of this otherwise extremely slow C−C bond forming reaction, with some enantioselectivity. Longer studies, 450 h, resulted in a proportional increase in the amount of product formed, which highlights the resilience of these materials to harsh environments.

Conclusions

The development of new methods for the catalysis of carbon−carbon bond formation remains one of the great challenges for synthetic organic chemistry. In this study we have demonstrated that molecularly imprinted polymers selective for a complex of Co^{2+} and a transition state analogue (**4**) for the aldol reaction of camphor (**1**) and benzaldehyde (**2**) can result in polymeric materials which increase reaction rate by a factor of over 50. Importantly, these polymers demonstrate enantioselective recognition of substrate and turnover. This study provides the first example of an enantioselective molecularly imprinted polymer capable of catalysis of carbon−carbon bond formation.

Experimental Section:

General. All reactions were performed under inert atmosphere. Benzaldehyde was freshly distilled before use. Benzoyl chloride was distilled from Ca and THF was dried over Na/benzophenone. MeOH was dried over I_2/Mg and freshly distilled prior to use. Divinylbenzene (DVB) was extracted three times with a solution of NaOH (0.1 M), dried over $MgSO_4$, filtered, and passed through basic Al_2O_3 before use. Azobis(cyclohexanecarbonitrile) (ABCC) was recrystallized from MeOH. Anhydrous DMSO (99.9%), anhydrous DME (99.5%), (*R*)-camphor (98%), (*S*)-camphor (99%), ethyl benzoate (99%), sodium hydride (95%), styrene (99%), 4-vinylpyridine (95%), *n*-BuLi (2.5 M in toluene), and $Co(OAc)_2 \cdot 4H_2O$ were used as received.

^1H and ^{13}C NMR spectra were recorded at 500, 400, 270, or 250 MHz and 125, 100, 68, or 63 MHz, respectively. $CDCl_3$ and C_6D_6 were used as solvents, and the signals of the solvents served as internal standards. Signals of methyl, methylene, and quaternary carbon atoms were distinguished by DEPT experiments. Homonuclear ^1H connectivities were determined by using COSY experiments. Heteronuclear $^1H-^{13}C$ connectivities were determined by using HSQC and HMBC experiments. Absolute configurations were resolved by NOESY experiments. Chemical shifts (δ) are reported in ppm and *J* values are presented in hertz. Mass spectra of positive ions obtained by electron impact (EI, 70 eV) were measured with an Agilent 6890 GC-system with a Agilent 5973 MS detector. FT-IR spectra were recorded with samples dispersed in KBr on a Nicolette Avatar FT-IR spectrophotometer by diffuse reflectance IR spectroscopy. VIS studies were performed on a Hitachi U2000 spectrophotometer. The data analyses were conducted with the software package Prism (version 3.03, GraphPad Software, USA).

(1*S*,4*R*)-(*E*)-3-Benzylidene-1,7,7-trimethylbicyclo[2.2.1]heptan-2-one (3a). To a cold (ice bath) solution of *n*-BuLi (2.5 M in toluene, 11 mL, 27.58 mmol) dissolved in DMSO (10 mL) was added dropwise a solution of (*S*)-camphor **1a** (3.00 g, 19.70 mmol) and benzaldehyde **2** (2.20 mL, 21.67 mmol) in DMSO (15 mL). The reaction mixture was stirred at room temperature overnight, then poured into ice water (250 mL) containing 10 mL of HOAc. The resulting yellow oil was extracted with Et_2O. The combined organic phases were dried ($MgSO_4$) and evaporated in vacuo. The crude yellow oil was recrystallized from EtOH to afford white crystals of **3a** (0.42 g, 9%). Mp 84−87 °C; $[\alpha]^{20}_D$ −369 (*c* 1.07, acetone); λ_{max} 290.0 (*c* 40 μM, log ϵ 4.38, MeOH); IR (KBr) 3024 (CH arom), 2956 (CH), 1720 (C═O), 1648 (C═C); ^1H NMR (400 MHz, $CDCl_3$, 25 °C) δ 7.50−7.48 (2H, d, $^3J = 7.3$, H^{3d}), 7.42−7.40 (2H, t, $^3J = 7.3$, H^{3e}), 7.38−7.34 (1H, d, $^3J = 7.3$, H^{3f}), 7.25 (1H, s, H^{3b}), 3.12−3.10 (1H, d, $^3J = 4.2$, H^4), 2.22−2.17 (1H, tt, $^3J = 4.2$, $^3J = 11.5$, $H^{5'}$), 1.83−1.76 (1H, dt, $^3J = 11.5$, $^3J = 2.8$, $H^{6'}$), 1.64−1.50 (2H, m, $H^{6''}$ and $H^{5''}$), 1.04 (s, 3H, Me^1), 1.01 (s, 3H, $Me^{7'}$), 0.81 (s, 3H, $Me^{7''}$); ^{13}C NMR (63 MHz, $CDCl_3$, 25 °C) δ 208.7 (C═O), 142.5 (C^{3a}), 136.1 (C^{3c}), 130.2 ($C^{3d}H$), 129.1 ($C^{3f}H$), 129.0 ($C^{3e}H$), 127.9 ($C^{3b}H$), 57.5 (C^7), 49.6 (C^4H), 47.1 (C^1), 31.1 (C^6H_2), 26.4 ($C^{5'}H_2$), 21.0 ($C^{7''}H_3$), 18.7 ($C^{7'}H_3$), 9.7 (C^1H_3); MS 240 (M^+, 100%), 225, 212, 197, 184, 169, 157, 141, 128, 115, 103, 91, 77, 55, 41. Anal. Calcd for $C_{17}H_{20}O$: C, 84.96; H, 8.39. Found: C, 85.27; H, 8.47.

(1*R*,4*S*)-(*E*)-3-Benzylidene-1,7,7-trimethylbicyclo[2.2.1]heptan-2-one (3b). The same procedure as for **3a** was employed, but with **1b** as starting material. CH_2Cl_2 was used for the extraction of **3b**, which was isolated as white crystals (0.44 g, 9%). Mp 95−97 °C; $[\alpha]^{20}_D$ +412 (*c* 1.00, acetone); λ_{max} 289.0 (*c* 40 μM, log ϵ 4.30, MeOH); IR (KBr) 3026 (CH arom), 2953 (CH), 1723 (C═O), 1650 (C═C); ^1H NMR (400 MHz, $CDCl_3$, 25 °C) δ 7.50−7.48 (2H, d, $^3J = 7.3$, H^{3d}), 7.42−7.39 (2H, t, $^3J = 7.4$, H^{3e}), 7.36−7.34 (1H, d, $^3J = 7.2$, H^{3f}), 7.25 (1H, s, H^{3b}), 3.13−3.12 (1H, d, $^3J = 4.2$, H^4), 2.24−2.16 (1H, tt, $^3J = 4.5$, $^3J = 11.5$, 5′), 1.83−1.76 (1H, dt, $^3J = 12.1$, $^3J = 3.0$, $H^{6'}$), 1.64−1.50 (2H, m, $H^{6''}$ and $H^{5''}$), 1.04 (s, 3H, Me^1), 1.01 (s, 3H, $Me^{7'}$), 0.81 (s, 3H, $Me^{7''}$); ^{13}C NMR (63 MHz, $CDCl_3$, 25 °C) δ 208.7 (C═O), 142.5 (C^{3a}), 136.1 (C^{3c}), 130.2 ($C^{3d}H$), 129.1 ($C^{3f}H$), 129.0 ($C^{3e}H$), 127.9 ($C^{3b}H$), 57.5 (C^7), 49.6 (C^4H), 47.1 (C^1), 31.1 (C^6H_2), 26.4 ($C^{5'}H_2$), 21.0 ($C^{7''}H_3$), 18.7 ($C^{7'}H_3$), 9.7 (C^1H_3); MS 240 (M^+, 100%), 225, 212, 197, 184, 169, 157, 141, 128, 115, 103, 91, 77, 55, 41. Anal. Calcd for $C_{17}H_{20}O$: C, 84.96; H, 8.39. Found: C, 85.05; H, 8.30.

(1*S*,3*S*,4*S*)-3-Benzoyl-1,7,7-trimethylbicyclo[2.2.1]heptan-2-one (4a). A solution of (*S*)-camphor **1a** (2.00 g, 13.1 mmol) dissolved in DME (12 mL) was added to a suspension of NaH (1.13 g, 47.3 mmol) in DME (18 mL). The mixture was refluxed for 1 h, whereupon ethyl benzoate (2.17 g, 14.6 mmol) dissolved in 12 mL of DME was added to the reaction mixture under reflux. After being stirred at reflux temperature overnight, the reaction was quenched by addition of 10 mL of EtOH (95%). The mixture was poured onto 60 mL of water and acidified with HCl until pH 1. The aqueous phase was extracted with pentane (3 × 75 mL). The combined organic phases were washed with an aqueous solution of $NaHCO_3$ (5%, 75 mL) and brine (75 mL). After drying of the organic phase over $MgSO_4$ and evaporation of the solvents, the yellow crude crystals were recrystallized from pentane to give **4a** as pale yellow crystals (1.38 g, 42%). Mp 65−67 °C; $[\alpha]^{20}_D$ −268 (*c* 0.99, CH_2Cl_2); λ_{max} 309.4 (*c* 80 μM, log ϵ 4.38); IR (KBr) 3200−2600 (br OH), 3051 (CH arom), 2968 (CH), 1663 (C═C), 1617 (C═O, β-diketone/enol); ^1H NMR (250 MHz, $CDCl_3$, 25 °C) (both diketo and keto−enol forms) δ 8.63 (0.3H, br s, OH-enol), 7.68−7.64 (2H, m, H arom), 7.43−7.42 (3H, m, H arom), 2.85−2.83 (0.7H, d, $^3J = 3.8$, OCCHCO), 2.22−2.11 (1H, m, CH, $CHC(CH_3)_2$), 1.83−1.74 (1H, m, CH), 1.67−1.48 (3H, m, CH_2 and CH), 1.02 (3H, s, CH_3), 0.94 (3H, s, CH_3), 0.82 (3H, s, CH_3); ^{13}C NMR (66 MHz, $CDCl_3$, 25 °C) (diketo and keto−enol forms) δ 213.2, 212.8, 210.6, 197.2, 193.3 (all C═O and C═C(OH)$_{keto-enol\ 2}$), 161.8 (C═C(OH)$_{keto-enol\ 1}$), 136.4, 134.1 (both C_q arom), 133.4, 133.1, 130.3, 129.9, 128.7, 128.3, 128.1, 127.8 (all CH arom), 115.4 (C═C(OH)$_{keto-enol\ 2}$), 63.8, 58.8 (both CH), 57.7, 57.6, 50.0 (both C_q), 48.6, 48.4 (both CH), 46.4, 46.3 (both C_q), 45.2 (CH), 30.6, 30.2, 28.9, 27.9, 27.1, 22.1 (all CH_2), 21.6, 20.3, 19.7, 19.6, 18.9, 18.8, 9.6, 8.8 (all CH_3); MS 256 (M^+), 241, 228, 213, 196, 185, 171, 147, 135, 123, 105 (100%), 91, 77, 55, 41. Anal. Calcd for $C_{17}H_{20}O_2$: C, 79.65; H, 7.86. Found: C, 80.10; H, 7.96.

(1*R*,3*R*,4*R*)-3-Benzoyl-1,7,7-trimethylbicyclo[2.2.1]heptan-2-one (4b). The same procedure as for **4a** was employed, with the (*R*)-camphor **1b** as starting material. The product, **4b,** was isolated as pale yellow crystals (2.91 g 58%). Mp 84−86 °C; $[\alpha]^{20}_D$ +277 (*c* 1.00, $CHCl_3$); λ_{max} 306.0 (*c* 80 μM, log ϵ 4.08, MeOH); IR (KBr) 3200−2600 (br s, OH), 3057 (CH arom), 2959 (CH), 1669 (C=C), 1607 (C=O, β-diketone/enol); ^{1}H NMR (250 MHz, $CDCl_3$, 25 °C) (both diketo and keto−enol forms) δ 8.64 (0.15H, br s, OH-enol), 7.69−7.65 (2H, m, H arom), 7.45−7.43 (3H, m, H arom), 2.85−2.84 (0.87H, d, ^3J = 3.8, OCCHCO), 2.22−2.11 (1H, m, CH, CH*C*(CH_3)$_2$), 1.83−1.74 (1H, m, CH), 1.67−1.49 (3H, m, CH_2 and CH), 1.03 (3H, s, CH_3), 0.94 (3H, s, CH_3), 0.83 (3H, s, CH_3); ^{13}C NMR (66 MHz, $CDCl_3$, 25 °C) (diketo and keto−enol forms) δ 213.2, 212.9, 210.7, 197.2, 193.3 (all C=O and *C*=C(OH)$_{keto-enol\ 2}$), 161.8 (*C*=C(OH)$_{keto-enol\ 1}$), 136.5, 134.1 (both C_q arom), 133.4, 133.1, 130.3, 129.9, 128.7, 128.3, 128.1, 127.8 (all CH arom), 115.4 (C=*C*(OH)$_{keto-enol\ 1}$), 63.8 (C_q), 58.8 (CH), 57.7, 50.1 (both C_q), 48.6, 48.4 (both CH), 46.4, 46.3 (both C_q), 45.2 (CH), 30.6, 30.2, 28.9, 27.9, 27.1, 22.1 (all CH_2), 21.6, 20.3, 19.7, 19.6, 19.0, 18.8, 9.7, 8.9 (all CH_3); MS 256 (M^+), 241, 228, 213, 196, 185, 171, 147, 135, 123, 105 (100%), 91, 77, 55, 41. Anal. Calcd for $C_{17}H_{20}O_2$: C, 79.65; H, 7.86. Found: C, 79.45; H, 8.00.

Attempted Synthesis of (1*S*,3*R*,4*S*)-3-Benzoyl-1,7,7-trimethylbicyclo[2.2.1]heptan-2-one (5a). A solution of SmI_2 in THF (0.1 M) was prepared by adding THF (100 mL) to Sm (1.80 g, 12 mmol) and I_2 (2.54 g, 10 mmol) and stirring the reaction mixture vigorously at 22 °C overnight. The color of the reaction changed from brown to green and then to Prussian blue. Then, (*S*)-bromocamphor **7a** (1.15 g, 5 mmol) and benzoyl chloride (0.70 g, 5 mmol) were dissolved in THF (10 mL) and the solution was added slowly at 0 °C to the solution of SmI_2 in THF. The resulting brownish mixture was stirred at room temperature overnight. The solvent was evaporated and the residue was hydrolyzed with HCl (10 mL, 15%). The aqueous phase was extracted 3 times with Et_2O. The combined organic phases were dried over $MgSO_4$ and evaporated to give a brown oil containing **4a** and **5a** in a ratio of 2:1. Partial ^{1}H NMR spectrum of **5a** (250 MHz, $CDCl_3$, 25 °C) δ 4.25−4.22 (1H, dd, ^3J = 1.3, ^3J = 4.3, OCCHCO). Purification of the crude product by flash chromatography on silica gel (eluent: Et_2O/cyclohexane 1:6, triethylamine 1%) gave exclusively **4a**.

Attempted Synthesis of (1*R*,4*S*,4*R*)-3-Benzoyl-1,7,7-trimethylbicyclo[2.2.1]heptan-2-one (5b). The same procedure as for **5a** was employed but with the (*R*)-bromocamphor **7b** as starting material. The crude product was also isolated as a brown oil containing **4b** and **5b**. Partial ^{1}H NMR spectrum of **5b** (250 MHz, $CDCl_3$, 25 °C) δ 4.27−4.25 (1H, dd, ^3J = 1.2, ^3J = 4.8, OCCHCO). The crude product was purified by flash chromatography on neutral alumina (eluent: Et_2O/cyclohexane 1:6) to exclusively give **4b**.

NMR Titrations. A solution of **4a** (10 mM) and pyridine-d_5 (20 mM) in CD_3OD was titrated by consecutive additions of a solution containing $Co(OAc)_4 \cdot 4H_2O$ (40 mM), **4a** (10 mM), and pyridine-d_5 (20 mM) in CD_3OD. ^{1}H NMR spectra were recorded at 250 MHz at 298 K. CD_3OD (99.8%), pyridine-d_5 (99%), and $CDCl_3$ (99.9%) were used as solvents. Apparent dissociation constants were calculated with nonlinear line fitting to a one-site model where each regression was based on no less than 8 data points and results are presented with the standard error. The goodness of fit (R^2) was 0.9898 or better in all cases.

VIS Titrations. Formation of prepolymerization complexes was studied by titrating a solution of $Co(OAc)_2 \cdot 4H_2O$ (20 mM) in MeOH containing 40 mM pyridine with a solution of **4b** (80 mM) in MeOH containing 40 mM pyridine. The effect of the different components on complexation strength was elucidated by titrating a solution of $Co(OAc)_4 \cdot 4H_2O$ (10 or 5 mM) in MeOH with a solution of **4b** (40 mM) or pyridine (5000 mM) in MeOH. Job's method of continuous variation was employed for determining the stoichiometric relationship between Co^{2+} and **4b** in MeOH. The change in absorbance was recorded at 400−700 nm and apparent dissociation constants (app K_{diss}) were calculated by plotting the change in absorbance at 520 nm followed by fitting the data to a one-site binding model. The goodness of fit (R^2) was 0.9880 or better in all cases.

Polymer Synthesis. 4-Vinylpyridine (430 μL, 4.0 mmol), styrene (4580 μL, 40.0 mmol), and divinylbenzene (5690 μL, 40.0 mmol) were mixed with **4a** or **4b** (512.7 mg, 2.0 mmol), azobis(cyclohexanecarbonitrile) (ABCC) (293.2 mg, 1.2 mmol), and $Co(OAc)_4 \cdot 4H_2O$ (498.2 mg, 2.0 mmol) in MeOH (14.98 mL), and briefly sonicated. The mixture was degassed by repeated freeze−thaw cycles (three times) and after the last cycle left under vacuum. Polymerization was carried out at 55 °C (36 h) to obtain polymers **P2** (**4a**) and **P3** (**4b**). The bulk polymers were ground and sieved through a 63 μm sieve and then wet sieved (acetone) through a 25 μm sieve. Particles in the range of 63−25 μm were collected. The fine particles were removed by repeated sedimentation from acetone (6 × 400 mL). The print molecule complex (**4a**-Co^{2+} and **4b**-Co^{2+}, respectively) was removed by packing the polymer (4 g) in an HPLC column and washing with acetic acid/MeOH 7:3 (400 mL), MeOH (100 mL), 45 mM Na_2-EDTA in MeOH/water (400 mL), MeOH (50 mL), and acetone (100 mL). Two reference polymers were also synthesized as described above, **P0** (absence of **4** and Co^{2+}) and **P1** (absence of **4**).

Polymer Titrations. To duplicate samples of blank polymer (**P0**) and (*R*)-MIP (**P3**) (1 to 20 ± 0.05 mg) solutions of 0.1 or 0.015 mM of **4b**:Co^{2+} (1:1) in MeOH were added and the samples were incubated at room temperature for 19 h. The samples were filtered trough 13 mm syringe filters with 0.2 μm PTFE membranes and analyzed on a Kromasil C18 column (5 μm 150 mm × 4.6 mm) at 295 nm on a HP 1050 HPLC with the mobile phase MeOH/water (9:1) and the flow 1.0 mL/min.

Batch Binding Studies. On the basis of the polymer titration results, batch binding studies were performed in MeOH or DMF, using 20 mg of polymer (**P0**, **P1**, **P2**, and **P3**) and various ligands (**2, 3a, 3b, 4a**, and **4b**), 0.015 mM. All samples were incubated for 19 h at room temperature. Determinations of bound ligand were performed as described above. All studies were performed in at least duplicate, with duplicate analysis of all points.

Reaction Assays. Polymer assays were performed according to Matsui et al.[14] with minor modifications. Polymer samples (**P0**, **P1**, **P2**, and **P3**) were incubated at room temperature for 19 h with $Co(OAc)_4 \cdot 4H_2O$ (1 mg/100 mg of polymer) in MeOH (0.5 mL). The samples were filtered and the concentration of bound Co^{2+} was established by analysis of the residual Co^{2+} present in the filtrate by quantitative spectrophotometric analysis (520 nm). The polymers were then dried under vacuum overnight at room temperature. Cobalt treated polymer samples (200 mg) were incubated with **1a** or **1b** (200 μmol) and **2** (200 μmol) in dry DMF (1.0 mL). Solution reactions were carried out as above with pyridine (10 μL) and $Co(OAc)_4 \cdot 4H_2O$ (8 μmol). The reactions were performed in sealed tubes at 100 °C in a thermostated oil bath. Samples (10 μL) were taken directly from the reaction mixtures and diluted 100-fold before filtration and analysis by HPLC, using a Kromasil C18 5 μm 150 mm × 4.6 mm column at 295 nm. HPLC analyses were run isocratically with MeOH/water (9:1) as the mobile phase at 1.0 mL/min. Standard curves of concentration versus peak area were prepared in triplicate over the concentration ranges used in the assay for calculation of the product yield.

Inhibition Studies. Samples were prepared in triplicate with $Co(OAc)_4 \cdot 4H_2O$ treated polymer (**P2**) (200 mg) incubated with **1a** (100 μmol) and **2** (50 to 400 μmol) in dry DMF (0.5 mL). As controls, solution reactions were carried out as described above. Inhibition was performed by addition of 0, 5, and 20 mM of **6**. The reactions were performed in sealed tubes at 100 °C in a thermostated oil bath. Samples (10 μL) were taken directly from the reaction mixtures and diluted 100-fold before filtration and analysis by HPLC, using a Kromasil C18 5 μm 150 mm × 4.6 mm column at 295 nm. HPLC analyses were run isocratically with MeOH/water (9:1) as the mobile phase at 1.0 mL/min.

Acknowledgment. We thank Dr. Jesper G. Karlsson (University of Kalmar, Sweden), Hannu Luukinen (University of Oulu, Finland), and Dr. Mats Malmberg (Synthelec AB, Sweden) for assistance with NMR measurements. We also thank Dr. Håkan S. Andersson (University of Kalmar, Sweden) and Dr. Michael J. Whitcombe (Cranfield University, UK) for fruitful discussions. The financial support of the Swedish Research Council (VR), National Research School in Pharmaceutical Sciences (Fläk), Swedish Knowledge Foundation (KKS), and the University of Kalmar is most gratefully acknowledged.

Supporting Information Available: Spectroscopic data (NMR) for synthesis products, proposed mechanism for keto−enol tautomerism, additional spectroscopic titration data, additional binding study data, and polymer swelling studies. This material is available free of charge via the Internet at http://pubs.acs.org.

JO060608B